

## **EXPERIMENTAL MEASUREMENTS AND NUMERICAL NON- LINEAR SIMULATION OF THE IN-PLANE BEHAVIOUR OF R/C FRAMES WITH MASONRY INFILLS UNDER CYCLIC EARTHQUAKE-TYPE LOADING**

**George C. Manos<sup>1</sup>, Vassilios J. Soulis<sup>2</sup>**

<sup>1</sup> Emeritus Professor, Department of Civil Engineering, Aristotle University of Thessaloniki,  
Thessaloniki, Greece  
[gcmayos@civil.auth.gr](mailto:gcmayos@civil.auth.gr)

<sup>2</sup> Lecturer Department of Civil Engineering, Technical Educational Institute of Piraeus, Piraeus,  
[vassilios\\_soulis@yahoo.com](mailto:vassilios_soulis@yahoo.com)

**Keywords:** Numerical simulation, Masonry-infilled R/C frames, Flexural and Shear failure of columns.

**Abstract.** *Masonry infills within multi-story reinforced concrete (R/C) framed structures were damaged to a considerable extend during past strong earthquake activity. The realism of numerically simulating the cyclic earthquake-type behaviour of masonry infilled R/C frames was studied extensively in the past by comparing numerical predictions with results from a series of pseudo-dynamic tests on masonry infilled R/C frame specimens. An advanced non-linear 2-D numerical simulation was validated which can realistically capture the in-plane hysteretic behaviour of reinforced concrete (R/C) frames with masonry infills when subjected to combined in-plane vertical and cyclic seismic-type horizontal load. Observations of failure modes for R/C infilled frames with columns under-designed in shear have shown that, when subjected to earthquake loads, the development of shear failure for the columns is an additional realistic scenario. The advanced non-linear 2-D numerical simulation is extended here to include both flexural and shear modes of failure for the R/C columns resulting from the interaction of the masonry infill with the R/C frame. A macro-model have been adopted for the numerical simulation of the masonry infill that retains the non-linear behaviour of the masonry infill itself as well as the non-linear behaviour at the contact area between the masonry-infill and the surrounding frame. Next, the effectiveness of a micro-modeling numerical approach is also examined for simulating the behaviour of masonry infill within a R/C frame when different types of openings are present in the masonry infill. The results from three framed masonry infill specimens that were tested under horizontal cyclic loading at have been also utilized for the validation of this micro-modeling approach. Both simulation strategies were quite successful in predicting the observed response in terms of stiffness, strength, and modes of failure for either the masonry or the R/C frame*

## 1 INTRODUCTION

The interaction of the masonry infills and the surrounding frame has been a subject of research for quite some time. This problem is of practical significance when this type of structural assemblages, e.g. masonry infills and surrounding frames made of either reinforced concrete (R/C) or steel, are subjected to in-plane seismic forces. In this case the presence of the infill changes dramatically the overall in-plane stiffness and resistance of the R/C frame. This is the case till the masonry infill fails, being usually relatively weak ([1]).

An extensive experimental and numerical study ([2], [3], [4], [5], [6], [9], [10], [11]) was carried out at the laboratory of Strength of Materials and Structures, Aristotle University, in an effort to examine the in-plane seismic behaviour of infilled R/C frames. It was shown that the stiffness and strength of the examined masonry infilled, single-story R/C frames was significantly influenced by the following non-linear mechanisms:

- a) The non-linear flexural behaviour of the R/C frame (plastic hinges).
- b) The non-linear mechanisms that develop at the interface between the R/C frame and the masonry infill.
- c) The level of non-linear deformations that develop within the masonry infill itself.

Apart from the plastic hinges that develop at the ends of the R/C beam and columns, shear failure of under-designed columns was also observed. This is the rational for extending the 2-D advanced non-linear numerical approach to include the shear limit state for the R/C columns at predefined locations. In order to validate this development the experimental study conducted by Sariyannis [12] was utilized. In his study a number of one-storey one-bay 1/3 scaled infilled frames were subjected as was done in similar studies to combined loading; that is the application of constant amplitude axial forces at the columns and horizontal seismic type cyclic force at the level of the beam. Nine repaired infilled frames and two repaired bare frames were examined in this study. These specimens resulted by repairing the damaged R/C frames, tested previously by Stylianides [7], and by rebuilding new stronger masonry infills [12]. In a number of these repaired specimens tested by Sariyannis [12] the shear sliding of the infill along a horizontal mid-height mortar joint or the corner crushing of the masonry infill was accompanied by the shear failure of the adjacent R/C columns. Two of these masonry infilled frame specimens, namely F1NR and F8NR, failed as a result of corner crushing of the infill and shear failure of the column [12].

Stavridis [13], carried out an experimental study of quasi-static tests with single-bay, single-story, masonry-infilled, non-ductile RC frames, which were scaled sub-assemblages of a prototype structure. These tested specimens were 2/3-scaled models of characteristic frames of a prototype building with design details representative of those used in the construction practice in California during the 1920's [13]. Two of these specimens (referred to as CU1 and CU2) were single-story, single bay masonry infilled frames that were tested with quasi-static cyclic loads [9]. A third specimen represented a three storey frame with two bays; this was tested on a shaking table at UCSD [13]. After reaching the peak load, specimen CU1 developed diagonal shear cracks in the concrete columns as an extension of the dominant cracks in the masonry infill. The same failure pattern was reported for the CU2 specimen with a window opening. Again, one of the columns in the CU2 specimen had a major shear crack which developed close to mid-height of the column. Koutromanos et al. [14], demonstrated the ability of a proposed nonlinear finite element model to capture the response of masonry-infilled reinforced concrete frames under cyclic loads. Diffused cracking and crushing in concrete and masonry are simulated by a smeared-crack continuum model, while dominant cracks as well as masonry mortar joints are modeled with the cohesive crack interface model.

Penava, Sigmund, Kozar [15], studied various non-linear FEM modeling techniques for numerical simulation of framed-masonry structures under cyclic loading. Numerical results are validated utilizing experimental results of framed masonry specimens with or without openings. Penava et.al [16] tested 10 framed-masonry specimens of 1:2:5 scale. These test specimens were divided into three groups. The first group consisted of four R/C infilled frames with an unconfined opening, e.g. a door or window, either in the center of the infill or offset from the center. The specimens of the second group had a vertical tie element around the opening. The third group consisted of two R/C infilled frames, one without an opening and one “bare” reinforced concrete frame. Penava et al. [15] proposed a micro-model numerical approach and calibrated the assigned numerical parameters in order to obtain the best correlation between experimental and numerical results. The concrete parts were simulated employing plane stress elements. For the reinforced concrete frame (Columns and lintel) were modeled adopting the fracture-plastic constitutive law, known as the Non-Lin-Cementitious material model. The longitudinal and transverse steel reinforcement of the reinforced concrete frame were modeled utilizing truss elements. In their numerical simulation Panava et al. [15] followed a micro-modeling approach whereby the masonry units and the mortar-masonry interface were considered separately and, in this way, it was possible to capture the sequenced failure of the masonry infill wall and to avoid modeling of the mortar. In this micro-modeling approach the smeared crack method has been adopted for the modeling the behaviour of the masonry units. For each material, the most appropriate constitutive law capable of describing its structural behaviour was used. The contact between the masonry units, as well as between the masonry units and the frame (the mortar in the physical model), was described by the interface material model. This model is based on the Mohr–Coulomb criterion with tension cut-off and requires the determination of the initial elastic normal and shear stiffness. Penava et al. [15] showed that the best correlation between the numerical and experimental results was achieved when they combined measured material data, with the addition of a cohesion hardening-softening function for bed joints to take into account the mortar interlocking within the hollow part of the masonry unit.

A numerical micro-model was proposed by Lourenco and Rots [17] for masonry wall piers under combination of horizontal and vertical loads. In their simulation the masonry units were expanded by the masonry mortar thickness leaving all the non-linear behavior concentrated in the interface between units. In this current investigation the micro-model proposed for the masonry infill by Soulis [10] was utilized and validated against the experimental and numerical results of the frame masonry specimens tested by Penava et.al [16]. The measured material properties as obtained by normative tests by Penava et.al [16] were used in this case. Differences and similarities between the micro-model proposed by either Penava et al. [15] or by Manos and Soulj's are discussed in section. Shear failure of the frame columns' was not observed in the frame specimens tested by Penava et.al [16]. Therefore, the possible shear failure of column frame members is not simulated for these frames as was done for the frames tested by Saryiannis [12], and Stavridis [13].

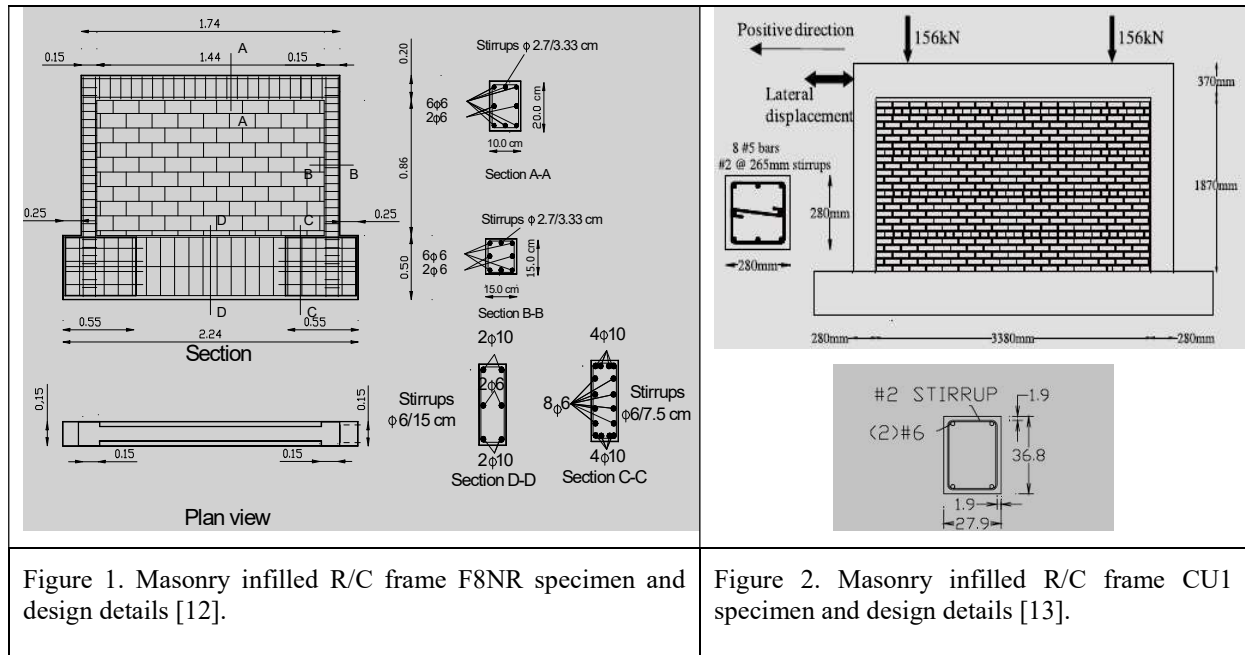
## 2. DESCRIPTION OF THE TESTED MASONRY-INFILLED R/C FRAMES

The macro-modeling numerical approach is first used to numerically simulate the measured behaviour of three masonry infilled frames; namely specimen F8NR, tested by Saryiannis [12], and specimens CU1, CU2, tested by Stavridis [13]. This numerical simulation includes the development of flexural plastic hinges and/or shear limit state at the surrounding R/C columns. The micro-modelling numerical approach is then used to numerically simulate the measured behaviour of specimens G1, G12, G12 [16]. Brief information on these selected

masonry infilled R/C specimens is given in table 1 and figures 1 and 2. Tables 2, 3 and 4 list the relevant mechanical properties. For all these specimens the numerical response predictions are compared with the corresponding experimental results. The influence exerted by the interface mortar joint between the masonry infill and the surrounding frame was examined in detail by Thauampteh [11] and Soulis [10].

Frame Code name	Vertical load on Columns (KN)	Technical description of masonry infill	Masonry Infill thickness (mm)	Technical description of the interface between frame and infill	Longitudinal reinforcement ratio ( $\rho$ )
F8NR <b>Repaired</b> [12]	80	Infill with mortar <b>O</b> reinforced with reinforced plaster, without transverse reinforcement	83	mortar <b>O</b> thickness <b>10mm</b> The reinforced plaster is in contact with the surrounding frame	1.01%
CU1[13]	156	Infill with mortar N	95	mortar N thickness <b>10mm</b>	1.00%
CU2[13]	156	Infill with mortar N	95	mortar N thickness <b>10mm</b>	1.00%
GII2 [16]	365	Infill with mortar <b>M5</b>	120	mortar <b>M5</b> thickness <b>10mm</b>	2.00%
GI1 [16]	365	Infill with central door and mortar <b>M5</b>	120	mortar <b>M5</b> thickness <b>10mm</b>	2.00%
GI2 [16]	365	Infill with central window and mortar <b>M5</b>	120	mortar <b>M5</b> thickness <b>10mm</b>	2.00%

Table 1 Outline of all specimens for the 1<sup>st</sup>, 2<sup>nd</sup> and 3<sup>rd</sup> group of specimens



Penava et. al [16] tested ten masonry infilled frame specimens of scale 1:2.5. The experimental behaviour of these masonry infilled frames under cyclic horizontal load was employed by Penava et. al [16] to calibrate their numerical model. Three of these masonry infilled frames, namely GI2, GI1, GII2, are studied currently towards validating the numerical simulation of masonry infilled frames applying the micro-modelling strategy proposed here and compare it with the micro-modelling approach proposed by Penava et. al [15, 16]. Brief information on these selected specimens GI2, GI1, GII2 is given in table 1 and figures 3 and 4. The mechanical properties of the reinforcement, masonry units and mortar joints are shown

in tables 2, 3, 5, 6, 7. Normative tests have been realized by Penava et al. [16] in a way similar to the one employed by Manos et al. [3] did to obtain the material properties. This was very useful in defining the mechanical properties assumed in these numerical simulations [3], [15].

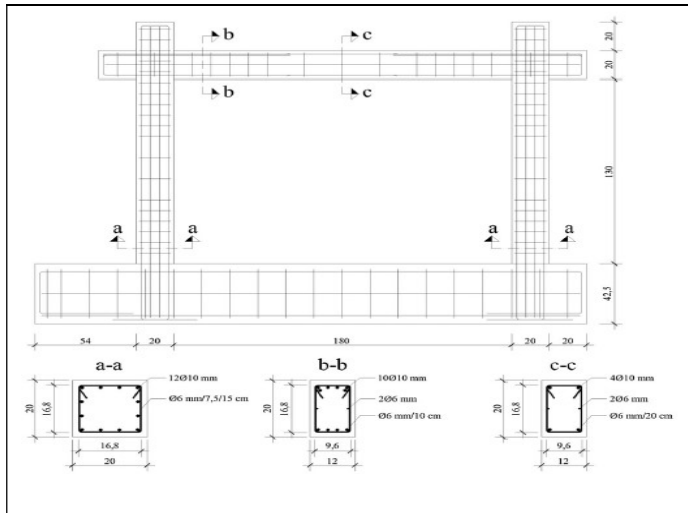


Figure 3. Bare R/C frame specimen and design details [16].

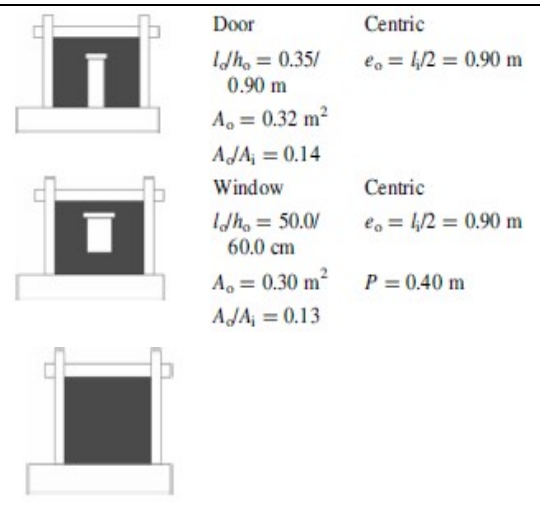


Figure 4. Masonry infilled R/C frames specimen and design details [16].

Masonry infill	Compressive strength of masonry (N/mm <sup>2</sup> )	Shear strength of masonry diagonal compression (N/mm <sup>2</sup> )	Compres. strength of masonry units (N/mm <sup>2</sup> )	Compres. strength of concrete (N/mm <sup>2</sup> )	Compres. strength of mortar cylinders (N/mm <sup>2</sup> )	Compres. strength of cement plaster (N/mm <sup>2</sup> )
Reinforced infill F8NR [12]						
Infill with mortar O, reinforced with reinforced plaster without transverse reinforcement	2.12	0.64 (corner crushing)	5.50	25.9	2.7	11.3
Virgin infill CU1, CU2 [13]						
Infill with mortar N	24.3		49	29,5	9.2	
Virgin infill GI1, GI2, GI2 [16]						
Infill GI1, GI2, GI2			2.80	58		

Table 2: Strengths of masonry infills and concrete used in the specimens [12],[13], [16]

A/α	Yield stress $f_{sy}$ (N/mm <sup>2</sup> )	Ultimate strength $f_{su}$ (N/mm <sup>2</sup> )	Strain at yield $\epsilon_{sy}$ (%)	Strain at ultimate stress $\epsilon_{su}$ (%)	Young Modulus (N/mm <sup>2</sup> )
Reinforced infill F8NR [12]					
Φ5.5	348	457	0.174	18.0	2X10 <sup>5</sup>
Φ2.7stirrups	271	395	0.135	19.0	2X10 <sup>5</sup>
Virgin infill CU1[13]					
Φ#5 15.9mm	472	752	-	9.0	
Φ#2 6.4mm stirrups	431	472	-	13.0	
Virgin infill GI1, GI2, GI2 [16]					
Φ10	550	650	1.0		2,1X10 <sup>5</sup>
Φ6stirrups	550	650	1.0		2,1X10 <sup>5</sup>

Table 3: Tensile strength of the reinforcement used in the specimens [12],[13],[16]

A/a	Simulation of joint interface between frame and infill	E Young Modulus (N/mm <sup>2</sup> )	G Shear Modulus (N/mm <sup>2</sup> )	f <sub>k</sub> Measured Compressive Strength of mortar (N/mm <sup>2</sup> )	f <sub>m</sub> Assumed Tensile Strength of mortar (N/mm <sup>2</sup> ) (as % of f <sub>c</sub> )	τ <sub>o</sub> Local bond shear strength of mortar (N/mm <sup>2</sup> )	μ friction coefficient
1	O mortar F8NR	540	234	2.70	0.27(10%)	0.31	0.58
2	N mortar CU1	1350	587	9,00	0.50		0.90
3	N mortar CU2	810	352		0,40		0.90

Table 4: Mechanical properties of the mortar joint located between the infill and the surrounding frame (mortar type H, N) [12], [13]

Initial masonry units properties adopted by Penava, Sigmund, Kozar[16]	Young Modulus parallel to head joints (N/mm <sup>2</sup> )	Young Modulus parallel to bed joints (N/mm <sup>2</sup> )	Tensile strength of masonry units parallel to head joints (N/mm <sup>2</sup> )	Compres. strength of masonry units parallel to head joints (N/mm <sup>2</sup> )	Strain at ultimate compressive strength ε <sub>c</sub>	Compres. strength of masonry units parallel to bed joints (N/mm <sup>2</sup> )
Infill GI1, GI2, GII2	5650	850	1,8	17.5	1.358 x10 <sup>-3</sup>	2.80

Table 5: Mechanical properties of the mortar units used by Penava et al [16]

Initial properties of bed joint adopted by Penava et.al [16]	Young Modulus (N/mm <sup>2</sup> )	Shear Modulus (N/mm <sup>2</sup> )	Compressive Strength of mortar (N/mm <sup>2</sup> )	Tensile Strength of mortar (N/mm <sup>2</sup> )	Local bond shear strength of mortar (N/mm <sup>2</sup> )	Friction coefficient
<b>M5</b> mortar	5650	2570	2.70	0.2	0.35	0.24

Table 6: Mechanical properties of the mortar bed joints used by Penava et al [16]

Simulation of head joint for masonry infilled R/C frames GI1, GI2, GII2						
Initial properties of head joint adopted by Penava, Sigmund, Kozar[16]	Young Modulus (N/mm <sup>2</sup> )	Shear Modulus (N/mm <sup>2</sup> )	Compressive Strength of mortar (N/mm <sup>2</sup> )	Tensile Strength of mortar (N/mm <sup>2</sup> )	Local bond shear strength of mortar (N/mm <sup>2</sup> )	Friction coefficient
<b>M5</b> mortar	850	386	2.70	0.2	1,05 *	0.24

\*Cohesion hardening –softening function

Table 7: Mechanical properties of the mortar head joints used by Penava et al [16]

### 3 THE NUMERICAL SIMULATION OF THE BEHAVIOUR OF SINGLE-STORY SINGLE-BAY MASONRY-INFILLED R/C FRAMES

#### 3.1 Numerical simulations of single story masonry infilled R/C frames

An extensive study on various numerical simulations of the behaviour observed for masonry infilled R/C one-bay one-storey frame specimens tested by Stylianides [7], Valiasis [8], Yasin [9], and by Thauampteh [11] was included in [10] together with an extensive validation process, utilizing the results of numerous experimental studies ([3], [7], [8], [9], [11]). Two different modelling strategies are applied here for the numerical simulation of the masonry infill, namely, a macro-modelling and a micro-modelling strategy. In macro-modelling strategy the masonry infills are simulated as plane stress elements with homogenised, single material properties (figure 5a). In micro-modelling strategy the constituents of the masonry infill are simulated separately (mortar bed, head joints, and masonry units, figure 5b), and different mechanical properties are assigned in each of these numerical representations. These two different numerical approaches were validated as described below:

a) The macro-modelling strategy was adopted for the simulation of the masonry infills of masonry infilled frame specimens F8NR and CU1, CU2 (figure 6a).

b) The micro-modelling strategy was adopted for the simulation of the masonry infills of masonry infilled frame specimens GI1, GI2, GII2 (figure 6b). This was partly dictated by the information on the material mechanical characteristics, which in this case were given for the masonry units and the mortar and not for the masonry that was built by these materials [16].

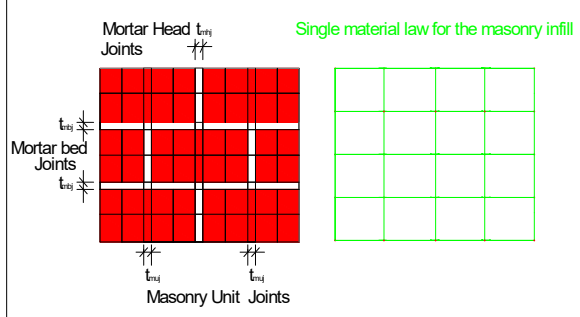


Figure 5a. Masonry infill simulation with macro-modelling strategy

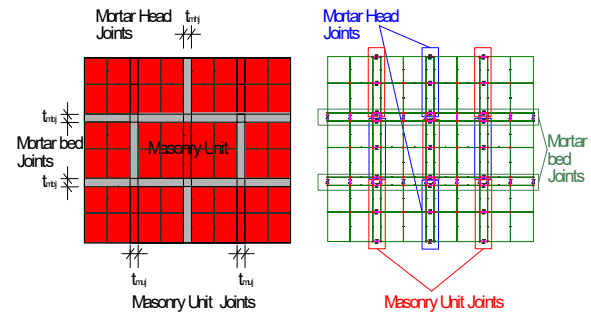


Figure 5b. Masonry infill simulation with micro-modelling strategy

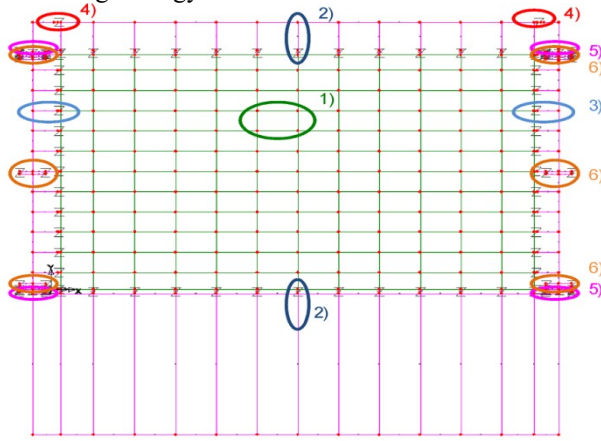


Figure 6a) Non-linear macro-model of a single-bay single-storey masonry infilled R/C frame



b) Non-linear micro-model of a single-bay single-storey masonry infilled R/C frame

For case a) an extension of the numerical simulation proposed by Soulis [10] was applied for specimens F8NR and CU1, CU2 capable of numerically simulating the formation of shear limit state in pre-defined locations along the height of the columns. The features of this numerical simulation are presented in figure 6a and in more detail in figures 7 and 8. These features are the same as the ones proposed by Manos, Soulis & Thauampthep before ([2], [3]) with the addition of the possibility of shear limit state at predetermined locations along the height of the R/C columns of the single storey R/C frame. In figure 6a, these non-linear mechanisms are denoted as: (1) corresponding to the non-linear behaviour of the masonry infill itself adopting a macro-model in this case, (2) the infill-beam interaction at the contact region, (3) the infill-column interaction at the contact region (4) the formation of a plastic hinge at the end of a beam, (5) the formation of a plastic hinge at the top or bottom of a column and finally (6) the formation of a shear limit state along the height of a column. These non-linear mechanisms are also depicted in some detail in figure 7 (non-linear mechanisms (1), (2), (3) and (4) and in figure 8 (non-linear mechanisms (5) and (6)). The modified Von Mises failure criterion with a softening post elastic behaviour was assumed for the masonry infills (1) adopting the macro-model.



For case b) the non-linear numerical simulation of the masonry infill frame specimens GI1, GI2, GII2 includes the same mechanisms (1), (2), (3), (4), (5) described above except the shear limit state of columns (6) as this failure mechanism was not observed during testing of these specimens. However, the prediction of shear failure on column elements can be incorporated in this case, if desired. In figures 9, 10, 11 the numerical simulation of masonry infilled frames GI1, GI2, GII2 is depicted.

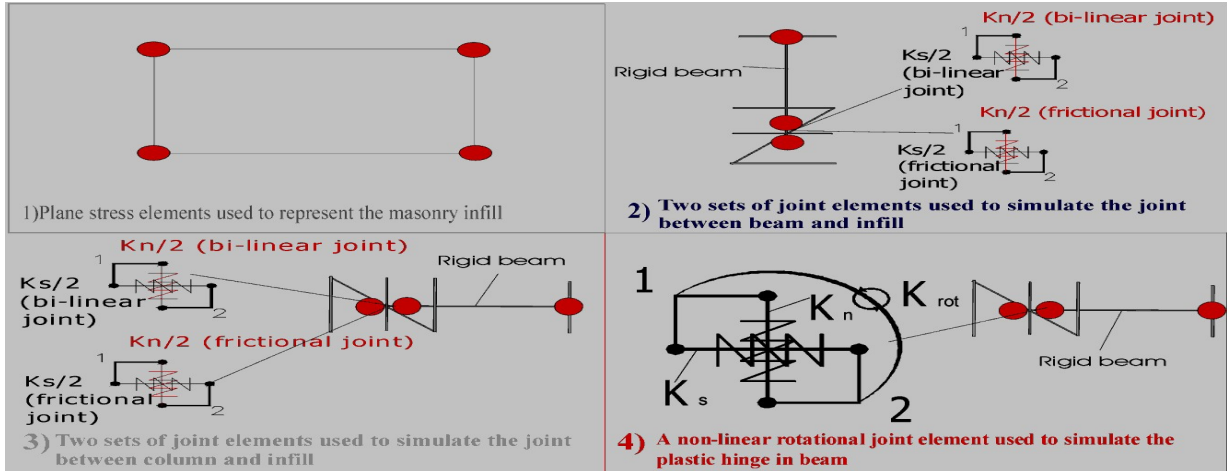


Figure 7. Details of the non-linear numerical simulation for the infill, the interface between infill and R/C frame and for the plastic hinge in the R/C beam.

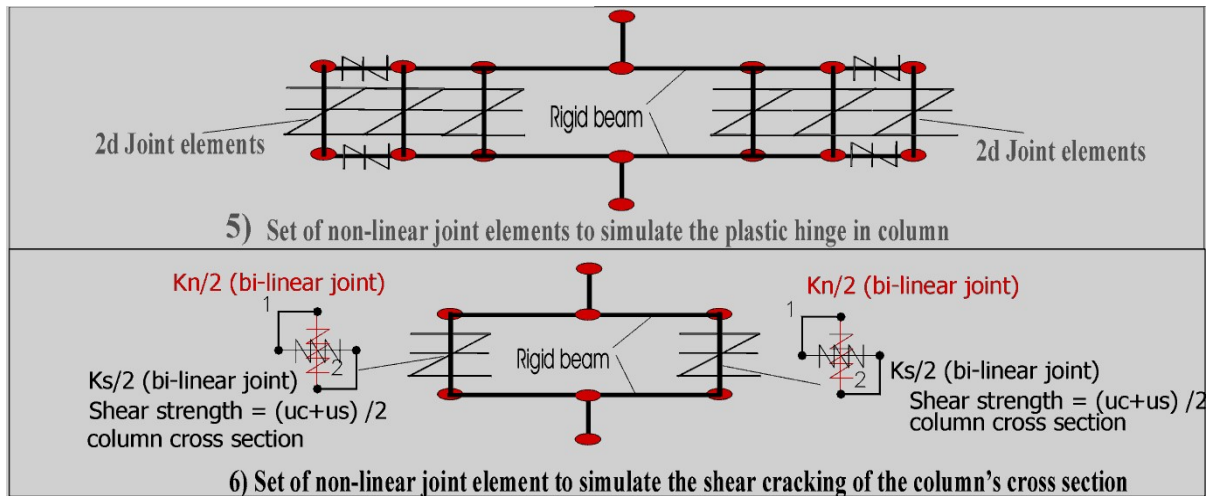


Figure 8. Details of the non-linear numerical simulation for the plastic hinge in the R/C column and for the shear limit state also at the column.

All these non-linear mechanisms are numerically simulated with a combination of rigid zones and non-linear joint elements (figures 7 and 8) with properties based on the geometric data, the material properties of the constituent materials (masonry, mortar, concrete, longitudinal steel) and the relevant structural detailing. Each one of the numerical simulations of the specific non-linear mechanisms (1) to (5) has been validated separately by Soulis [10] and Manos ([2], [3]) utilising relevant laboratory measurements obtained by Thauampth [11].





Figure 9. Non-linear micromodel of a single-bay single-storey masonry infilled R/C frame GII2

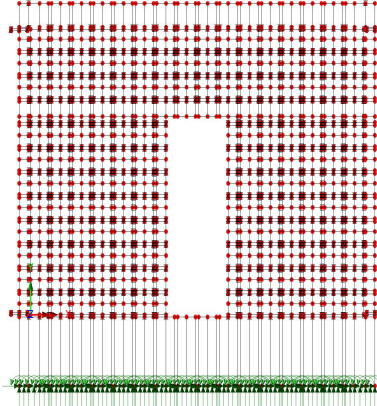


Figure 10. Non-linear micromodel of a single-bay single-storey masonry infilled R/C frame GI1

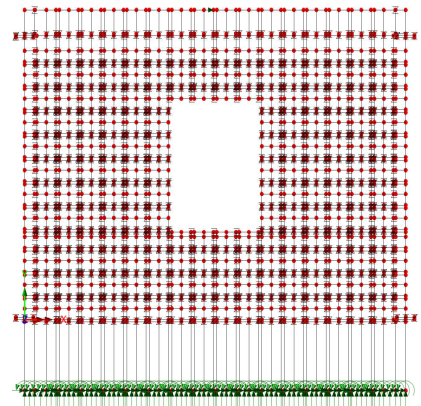


Figure 11. Non-linear micromodel of a single-bay single-storey masonry infilled R/C frame GI2

The additional shear limit state non-linear mechanism, represented by detail (6) in figure 6a, is numerically approximated again by a combination of rigid zones and non-linear joint elements with properties based again on the geometric data of the column cross section, the material properties of the constituent materials (concrete, transverse steel), and the relevant structural detailing. The shear limit state was obtained by calculating the shear capacity for a column cross-section as specified by equations 1, 2 and 3. The location of these non-linear shear limit state zones is based on observed behaviour and accumulated experience for each given case. For the studied specimens three predefined locations along the height of each column were selected capable of developing this shear limit state. Two of these locations are at the ends (top and bottom) of each column in serial sequence with the non-linear mechanism simulating the flexural plastic hinges in these locations. An additional shear limit state mechanism was also placed at mid-height of each R/C column. Two elasto-plastic non-linear 2-D joint elements are used to simulate the shear post-elastic behaviour of a given R/C column cross section by considering also the corresponding column transverse reinforcement (figure 6a and detail No 6 in figure 8).

$$V_u = V_c + V_s \quad (1)$$

- Shear resisted by the concrete part of the cross section  $V_c$
- Shear resisted by the transverse steel reinforcement  $V_s$

For normal weight concrete,

$$V_c = \delta \times (0.17 \times \sqrt{f'_c}) \times b \times d \quad (\text{where, } \delta = 1 + \frac{P_u}{14A_g}) \quad (2)$$

$$V_s = \frac{A_{sv} \times f_{yh} \times d}{s_v} \quad \text{for transverse reinforcement} \quad (3)$$

$f_c$  = cylindrical compressive strength of concrete  
 $b$  = width of member  
 $P_u$  = axial force normal to cross section  
 $A_g$  = gross cross sectional area of concrete

$A_{sv}$  = area of transverse steel reinforcement expected to be effective in resisting the expected shear mode of failure  
 $d$  = Effective depth of member  
 $s_v$  = spacing of stirrups  
 $f_{yh}$  = yield stress of stirrups

As per ACI 318:2008 [18] the total shear  $V_u$  resisted (**107KN**) by the column's cross section is composed by two parts; the shear resisted by the concrete and the shear resisted by the reinforcement. As already mentioned, the properties of these non-linear 2-D joint elements are specified utilizing the given structural details and equations 1 to 3. Independent numerical tests were carried out employing simple structural problems in order to verify that this way of simulating numerically the shear limit state mechanism responds in the expected way. Next, this numerical approach was applied to the infilled frame specimens F8NR, CU1 and CU2 .

### 3.2. Differences and Similarities of the Micro-Modelling Strategies

In what follows, the main differences and similarities in the modeling strategies as adopted by either Manos and Soulis or Penava et al. [15] are presented. It must be pointed out that in this discussion the features, the applicability and the validity of the results of the macro-modeling approach is not included, as it was presented in a number of past publication ([2], [3]). It should be underline the macro-modeling technique is generally simpler and less demanding in terms of computational cost. As was debated by Manos et al [2] even the simpler macro-modeling approach is in need of further simplification in order to numerically simulate multi-story R/C framed structures with masonry infills:

#### Reinforced concrete frame

- a) Penava et.al [15] utilizes instead plane elements to simulate the concrete volume. The non-linear behavior of the concrete was simulated adopting the fracture-plastic constitutive law which was assumed to be valid through all parts of the surrounding frame.
- b) Truss elements are used to model the longitudinal and transversal reinforcements in the numerical simulation by Penava et al. [15]. In addition, Penava et al. [15] assumed that the transverse reinforcement bar closest to the joint had to be moved further away from the joint edge, while its area was increased by about 100 times in order to prevent unrealistic tension softening. The combination of the numerical simulation of the concrete, as described in item a), with the longitudinal/transverse reinforcement is for general application, provided that the outcome can be checked for its realism in a qualitative and quantitative manner.
- c) The modelling strategy adopted by Soulis [10] utilizes linear elements for the simulation of the surrounding R/C frame. The flexural nonlinear behaviour of this frame is concentrated on predefined positions where plastic hinge formation is numerically simulated. A series of non-linear joint elements are mobilized to model this plastic hinge formation. This was extensively validated by Manos and Soulis [3, 10]. In this way, there is no distinct numerical simulation of the concrete volume and the longitudinal or transverse reinforcement separately. A similar approach is adopted for simulating the shear limit-state of the R/C columns. Again, a series of link elements are mobilized to numerically approximate shear limit-state at predetermined locations. This approach is of no general application as it requires engineering judgment for selecting the location for placing the non-linear mechanisms (a appropriate combination of non-linear links that is calibrated to have the desired non-linear properties) that will numerically simulate either the flexural or the shear limit state.
- d) As already mentioned, the numerical simulation adopted by Manos and Soulis does not deal to simulate separately longitudinal and/or transverse reinforcement. Instead, the flexural and shear limit states are numerically simulated at predetermined locations. These flexural and shear limit states are derived/calibrated from well validated experimental and analytical data and formulae combined with the relevant construction details and material properties of the given R/C cross sections.

Masonry infill

a) Both modeling strategies for the masonry infill utilize the micro-modeling technique. Masonry units and the mortar-masonry interface were considered separately. The mortar between masonry units was not modeled either in the numerical simulation of Pevana et al. or the numerical simulation proposed by Manos and Soulis. The masonry units are modeled as elastic plane stress elements with a non-linear joint interface in their centre in an effort to describe their quasi-brittle behaviour. This was done manually by introducing series of joint elements in the centre of a masonry unit element. Penava et al. [15] incorporated the SBeta material model that introduces automatically a rotated crack inside the simulation of plane masonry unit.

b) The contact between the masonry units, as well as between the masonry units and the surrounding frame was described with non-linear joint elements by Soulis [10] and with non-linear interface elements by Penava et al. [11]. These elements combine the Mohr-Coulomb failure criterion with a tension cut-off in both strategies. The bed and head joints were modeled adopting the mechanical properties defined by Penava et al. [15]. Normal and tangential stiffness of the bed joints in Soulis model [10] were calculated using the modulus of elasticity, the shear modulus and the poisson ratio as measured by Penava et al. [15]. The mortar interlocking in the hollow clay masonry units was simulated in both numerical simulations applying the cohesion-hardening-softening function as proposed by Penava et al. [15].

Joint interface between masonry infill and surrounding frame.

a) Non-linear joint elements used for the simulation of the interface between the masonry units and the surrounding frame in the investigation carried out by Manos and Soulis. The same mechanical properties that were used for the simulation of bed and head joints were also used for the simulation of the interface between masonry units and the surrounding frame. This selection was mutual for both models that were proposed by the two research groups (Manos and Soulis, and Penava et al. [11]).

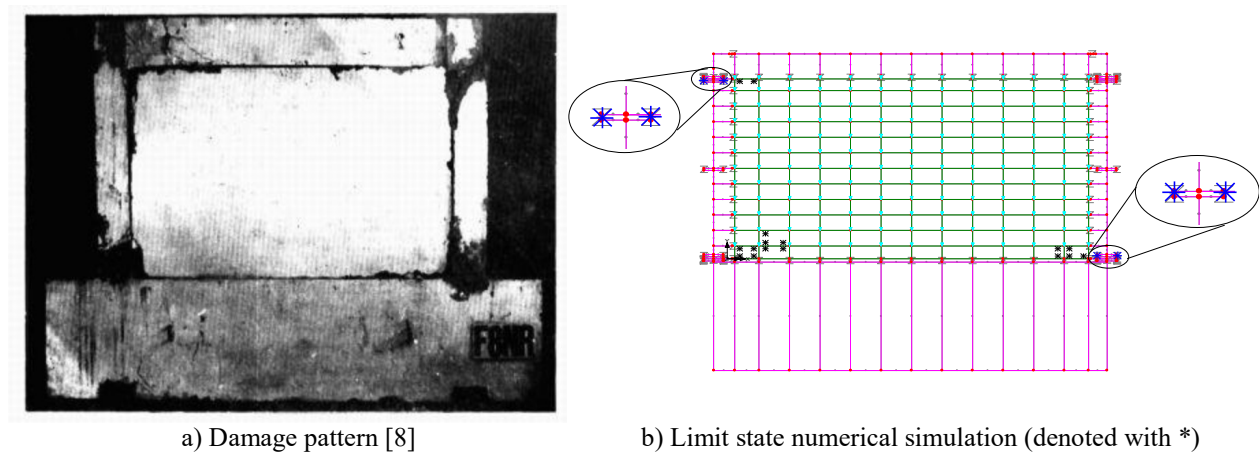
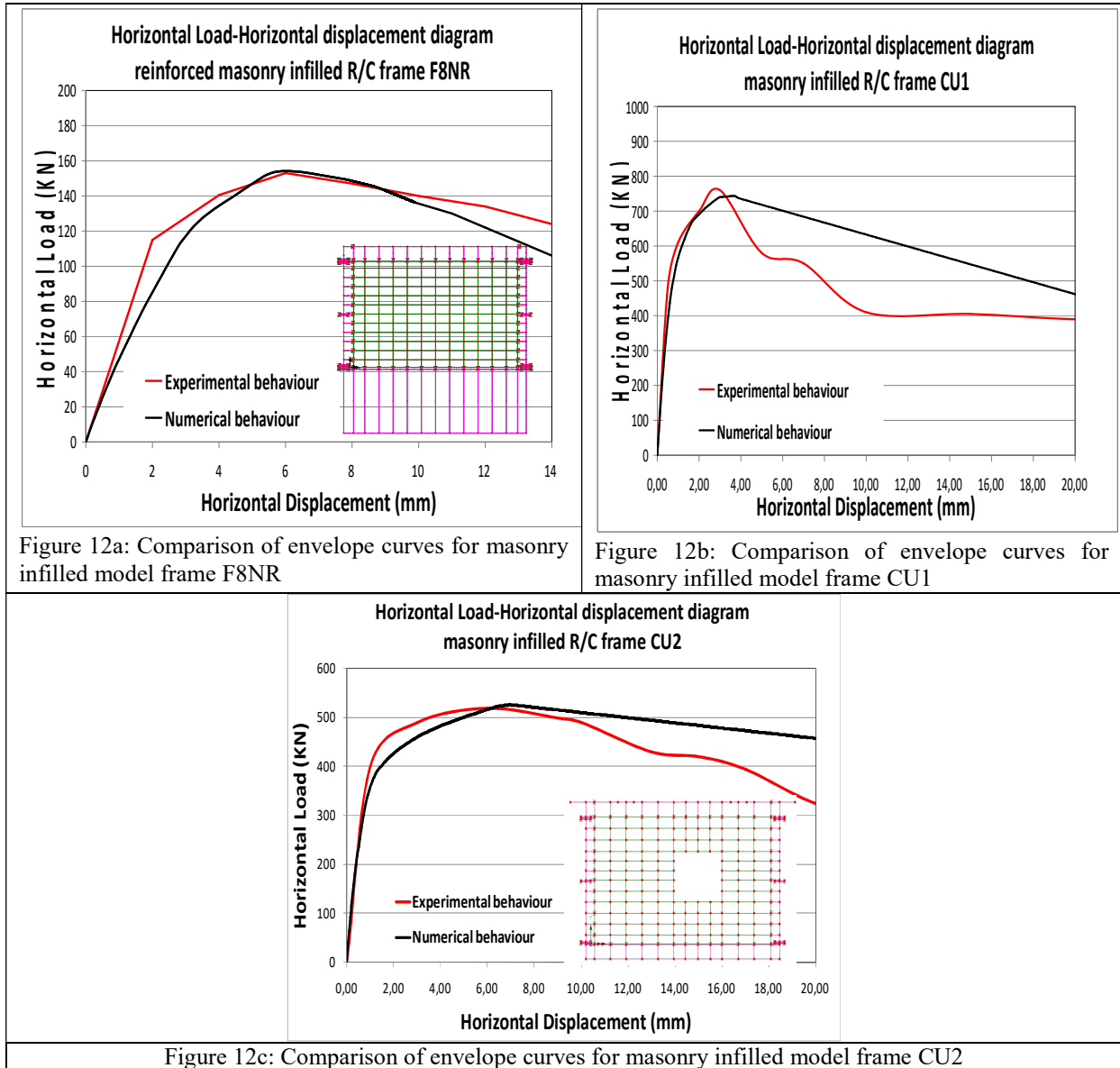
b) The non-linear behaviour of joint elements in the interface between the masonry infill and the surrounding frame were based on the Mohr-Coulomb criterion with tension cut off.

**3.3. Validation of the macro-modeling numerical simulations**

Figures 12a, 12b and 12c depict a comparison between the predicted behaviour by the macro-modeling approach, in terms of envelope curves resulting from a monotonic type of loading, and the corresponding envelope curves resulting from the relevant experiments on the masonry infilled frame specimens F8NR and CU1, CU2.

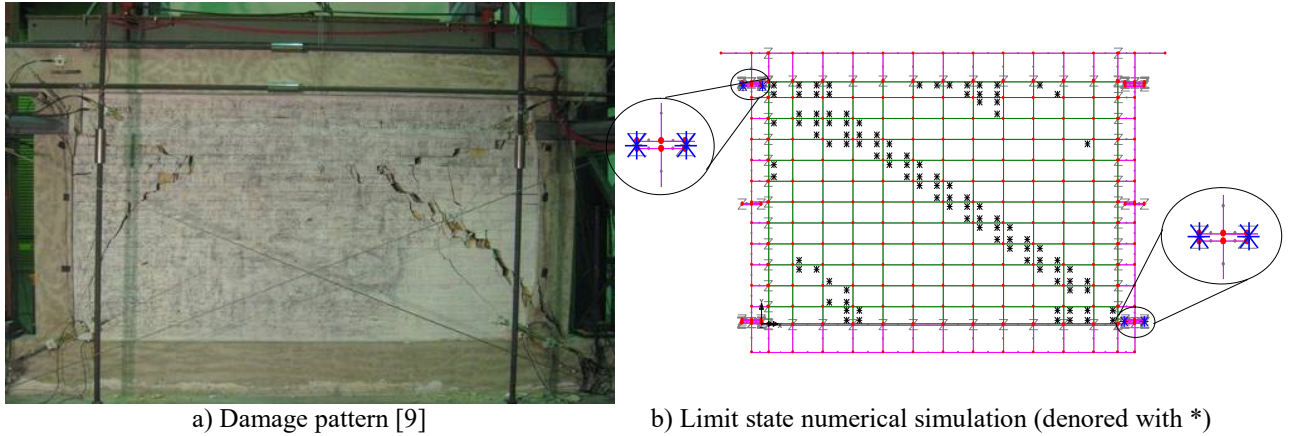
The damage pattern of the masonry infills observed during the tests and the numerically-predicted non-linear limit state is presented for frames F8NR (figures 13a and 13b), CU1 (figures 14a and 14b) and CU2 (figures 15a and 15b). The observed damage patterns of the masonry infills were well approximated by the proposed numerical simulation. The damage pattern of the tested F8NR masonry infilled R/C frame consisted of corner crushing of the reinforced masonry infill corners in the R/C column and beam joint and a shear cracking in top right column (figure 13a).

Reasonably good agreement can be seen in the damage pattern predicted numerically except that shear limit state is observed both in the top left and the bottom right column (figure 13b).



Figures 13 a) Damage pattern of masonry infill observed experimentally for infilled frame F8NR, b) Damage pattern(x) predicted numerically by the macro-modeling approach

The damage pattern that was observed for masonry infilled frame CU1 includes diagonal/sliding cracks in the infill panels and shear cracks on the top left column and shear cracks in the bottom right column for the experimentally tested specimen (figure 14a). The same limit state pattern was predicted numerically as shown in figure 14b. For the masonry infilled panel with one opening in specimen CU2 the sequence of limit states included successively (figure 15a) : a) Infill to frame separation b) diagonal cracks of the infill at the window corners c) shear crack in top left column , and d) diagonal crack in the right bottom masonry pier and shear crack mid-height of the right column. The same limit state pattern was predicted numerically (figure 15b). Further validation is included in [3] and [10].



Figures 14 a) Damage pattern of masonry infill observed experimentally for infilled frame CU1, b) Damage pattern(x) predicted numerically by the macro-modeling approach

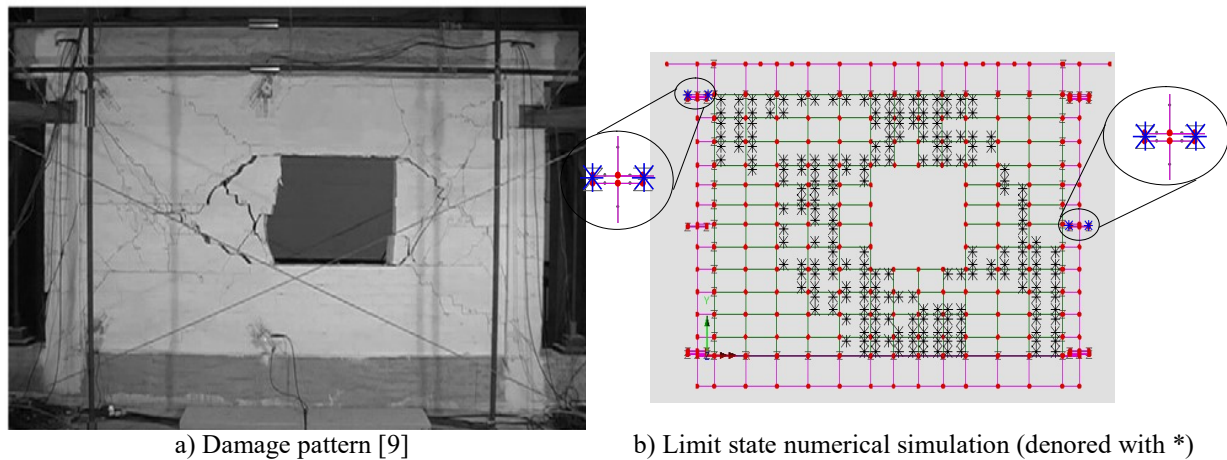


Figure 15 a) Damage pattern of masonry infill observed experimentally for infilled frame CU2, b) Damage pattern(x) predicted numerically by the macro-modeling approach

### 3.4. Validation of the micro-modeling numerical simulations

The comparison between the predicted behaviour, in terms of envelope curves resulting from a monotonic type of loading by the micro-modeling numerical simulation of the current study, the numerical simulation proposed by Penava et al. [15] and the corresponding envelope curves resulting from the relevant experiments of the masonry infilled frame specimens GII2, GI1 and GI2 is depicted in figure 16 a, 16b, 16c. In the case of masonry infilled frame with a central window opening GI2 (figure 16c), all numerical simulations underestimate the level of horizontal load that is obtained experimentally in the range of horizontal beam displacements



from 2mm to 6mm. For the other two specimens (GII2 and GI1) reasonably good agreement was obtained between all the numerical predictions and observed response.

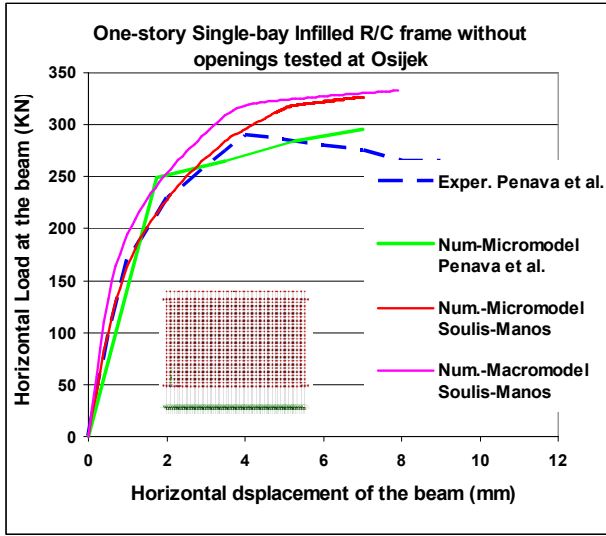


Figure 16 a) Comparison of envelope curves for masonry infilled model frame GII2

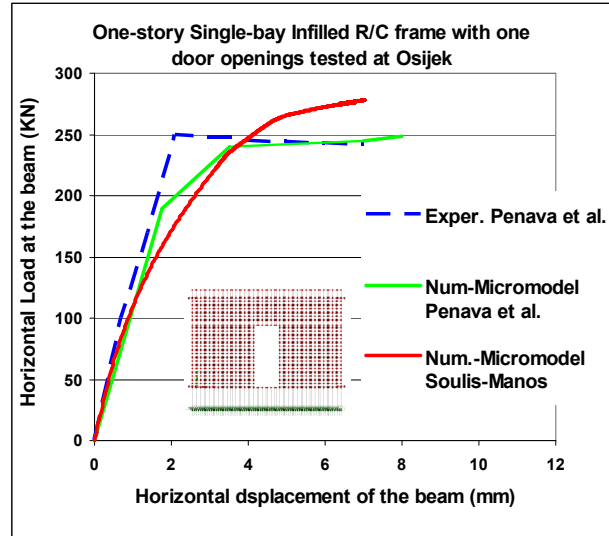


Fig. 16b) Comparison of envelope curves for masonry infilled model frame with central door opening GI1

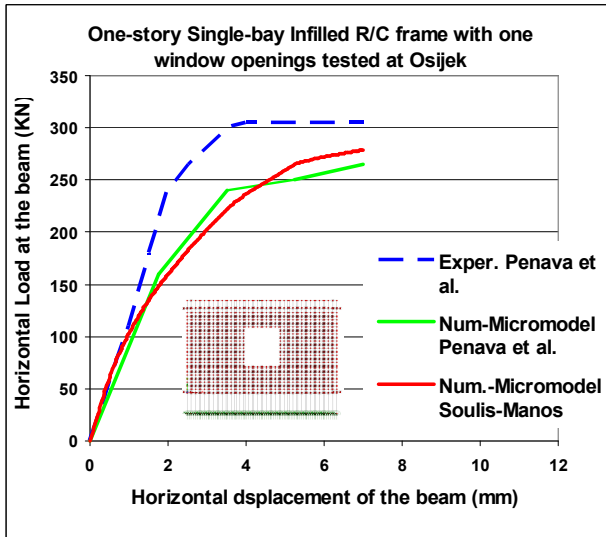

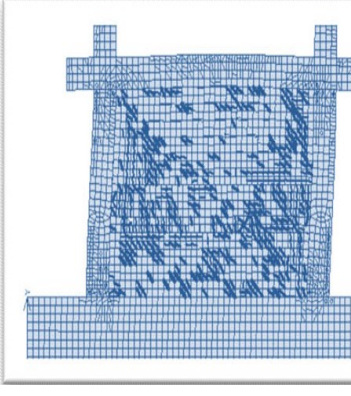
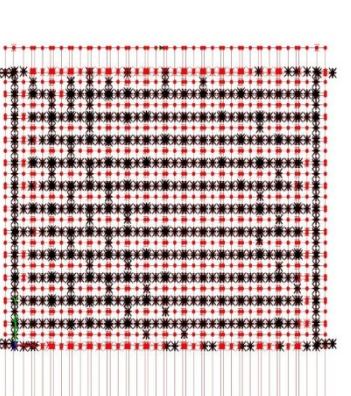

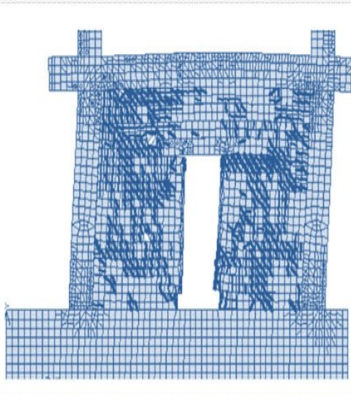
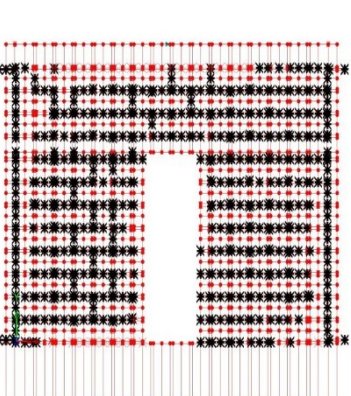

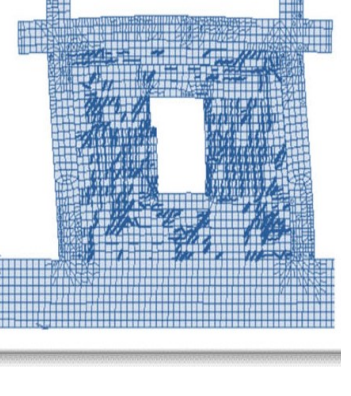
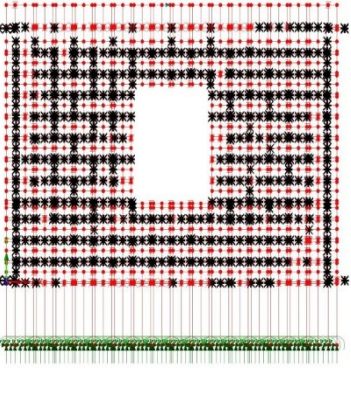


Figure 16c) Comparison of envelope curves for masonry infilled model frame with central window opening GI2

The damage patterns as observed experimentally are compared with the damage patterns predicted by the micro-modeling numerical simulations proposed by the authors in the current study and by Penava et.al [15]. In figure 17a), the damage pattern observed for the masonry infill frame GII2 without any opening is compared with the ones predicted numerically by Manos and Soulis micro-modeling (figure 17b) and Penava et.al [15] (figure 17c). The same comparison is repeated in figures 18a, 18b and 18c for the specimen GI1 with a door opening and in figures 19a, 19b and 19c for the specimen with one window opening.

The main characteristic in the observed damage in all three specimens is the diagonal failure of masonry infills and masonry piers. However, both micro-modelling numerical simulations show a wide distribution of failures that is not in full agreement with the observed damage.



		
<p>Figures 17 a) Damage pattern of masonry infill observed experimentally for infilled frame <b>GI12</b></p>	<p>b) Damage pattern(x) predicted numerically by Penava et.al [15] (micro-modelling)</p>	<p>c) Damage pattern(x) predicted numerically by Manos and Soulis micro-modeling approach</p>
		
<p>Figures 18 a) Damage pattern of masonry infill observed experimentally for infilled frame <b>GI1</b></p>	<p>b) Damage pattern(x) predicted numerically by Penava et.al [15] (micro-modelling)</p>	<p>c) Damage pattern(x) predicted numerically by Manos and Soulis micro-modeling approach</p>
		
<p>Figures 19 a) Damage pattern of masonry infill observed experimentally for infilled frame <b>GI2</b></p>	<p>b) Damage pattern(x) predicted numerically by Penava et.al [15] (micro-modelling)</p>	<p>c) Damage pattern(x) predicted numerically by Manos and Soulis macro-modeling approach</p>

## 4 CONCLUSIONS

1. The strength and the monotonic load-displacement behaviour observed during the experiments of Sariyannis [12] and Stavridis [13] on single-storey one-bay masonry-infilled R/C frames are successfully predicted by the proposed macro-modeling numerical simulation that includes both flexural and shear limit-states at predetermined locations for the R/C frame.
2. The proposed numerical simulation represents in a reasonable way the most important influences that the interface between masonry infill and the surrounding frame could exert on the monotonic behaviour of such structural assemblies in terms of stiffness, strength, modes of failure, as demonstrated from the observed behaviour.
3. The development of a shear limit state at the predetermined positions of columns of the surrounding R/C frame observed during the experiments as well as the damage patterns for the masonry infill, in terms of crack propagation are also successfully predicted.
4. The strength and the monotonic load-displacement behaviour observed during the experiments of Penava et.al [15] on single-storey one-bay masonry-infilled R/C frames including openings in their infills, are satisfactorily predicted by the micro-modeling numerical simulation proposed by Manos and Soulis in the current study. However, there is a discrepancy in the case of masonry infilled R/C frame with central window opening (GI2), where the horizontal bearing strength measured numerically is underestimated by the numerical simulation proposed.
5. In the current study the micro-modeling approach of Manos and Sulis was applied for the simulation of the masonry infills including openings tested by Penava et.al [15]. The differences and similarities with the micro-modeling technique adopted by Penava et.al [15] are commented and discussed. Both micro-modeling simulations predict common results in terms of the horizontal load -horizontal displacement curves and the predicted damage patterns.
6. The damage patterns predicted by this micro-modeling numerical simulation are in agreement with the damage patterns observed experimentally by Penava et.al [15]. However, both micro-modelling numerical simulations show a wide distribution of failures that is not in full agreement with the observed damage.
7. It must be pointed out that in this discussion the features, the applicability and the validity of the results of the macro-modeling approach are not included, as it was presented in a number of past publications ([2], [3]). It should be underline the macro-modeling technique is generally simpler and less demanding in terms of computational cost. As was debated by Manos et al [2] even the simpler macro-modeling approach is in need of further simplification in order to numerically simulate multi-story R/C framed structures with masonry infills.

## ACKNOWLEDGEMENTS

The assistance of the personnel of the laboratory of Experimental Strength of Materials and Structures of Aristotle University and Dr. J. Thauampteh in conducting the experimental sequence is gratefully acknowledged.

- To the memory of Ray W. Clough, Professor Emeritus of the University of California, at Berkeley, U.S.A.

## REFERENCES

- [1] Manos George, (2011), “Consequences on the urban environment in Greece related to the recent intense earthquake activity”, *Int. Journal of Civil Engineering and Architecture*, Dec. 2011, Volume 5, No. 12 (Serial No. 49), pp. 1065–1090.
- [2] Manos. G.C., Soulis V. J., J. Thauampth. “A Nonlinear Numerical Model and its Utilization in Simulating the In-Plane Behaviour of Multi-Storey R/C frames with Masonry Infills”, *The Open Construction and Building Technology Journal*, 6, (Suppl 1-M16) 254-277, 2012.
- [3] Manos. G.C., Soulis V.J., Thauampth J., “The Behaviour of Masonry Assemblages and Masonry-infilled R/C Frames Subjected to Combined Vertical and Cyclic Horizontal Seismic-type Loading”, *Journal of Advances in Engineering Software*, Vol. 45, pp. 213-231, 2011.
- [4] G.C. Manos, D. Naxakis, V. Soulis “The Dynamic and Earthquake Response of a two-story Old R/C Building with Masonry Infills in Lixouri-Kefalonia, Greece, Including Soil-Foundation Deformability”, *COMPdyn 2015*, Greece, 25–27 May 2015.
- [5] G. C. Manos and V. Soulis “Numerical Simulation of the non-linear in-plane seismic behaviour of masonry infills within Multi-story R/C Framed Structures, 12th North American Masonry Conference, Denver, Colorado, U.S.A. 17-20 May, 2015.
- [6] G.C. Manos & V. Soulis, (2016), “Numerical simulation of the non-linear behaviour of masonry infills within multi-story RC framed structures”, 2016 IBMac, Taylor & Francis Group, London, ISBN 978-1-138-02999-6, pp. 1253-1261.
- [7] Stylianides. K., “Experimental Investigation of the Behaviour of Single-storey Infilled R/C Frames under Cyclic Quasi-static Horizontal Loading (Parametric Analysis”, Ph.D. Thesis, Department of Civil Engineering, Aristotle University of Thessaloniki, 1985.
- [8] Valiasis. Th., “Experimental Investigation of the Behavior of R.C. Frames Filled with Masonry Panels and Subjected to Cyclic Horizontal Load - Analytical Modelling of the Masonry Panel”, Ph.D. Thesis, Department of Civil Engineering, Aristotle University of Thessaloniki, 1989.
- [9] Yasin, B., “Experimental Investigation of the Influence of Infills on the Dynamic Response of Building Structures Through the Study of Scaled Physical Models”, Ph.D. Thesis, Department of Civil Engineering, Aristotle University of Thessaloniki, 1999.
- [10] Soulis V.J. “Investigation of the Numerical Simulation of Masonry Infilled R/C Frame Structures under Seismic-type Loading”, Ph.D. Thesis, Department of Civil Engineering, Aristotle University of Thessaloniki, 2009.
- [11] Thauampth, J., “Experimental Investigation of the Behaviour of Single-storey R/C Frames with Masonry Infills, Virgin and Repaired, under Cyclic Horizontal Loading”, Ph.D. Thesis, Department of Civil Engineering, Aristotle University of Thessaloniki, 2009.
- [12] Sariyannis D., “Experimental Investigation On The Behaviour Of R/C Infilled Frames Repaired With Various Infill Techniques Under Cyclic Horizontal Loading” , Ph.D. Thesis, Department of Civil Engineering, Aristotle University of Thessaloniki, 1989.
- [13] Stavridis A., “Analytical and experimental study of seismic performance of reinforced concrete frames infilled with masonry walls”. PhD thesis. San Diego: Department of Structural Engineering, University of California; 2010.
- [14] I.Koutromanos , A. Stavridis, P. B. Shing, K. Willam, “Numerical modelling of masonry-infilled RC frames subjected to seismic loads” , *Computers and Structures* 89 (2011) ,pp 1026–1037

- [15] Penava. D, Sigmund V, Kozar. I, " Validation of a simplified micromodel for analysis of infilled RC frames exposed to cyclic lateral loads", Bull Earthquake Eng (2016) 14:2779–2804 DOI 10.1007/s10518-016-9929-0.
- [16] Penava D, "Influence of openings on seismic response of masonry infilled reinforced concrete frames, Josip Juraj Strossmayer University of Osijek, Osijek.
- [17] Lourenco P. Rots J.G, "On the use of micro-models for the analysis of masonry shear-walls" eds Pande G.N, Middleton J, Computer Methods in Structural Masonry-2, Swansea, UK, 1993, pp. 14-25.
- [18] ACI 318:2008, Building Code Requirements for Reinforced Concrete, American Concrete Institute, Detroit, Michigan, 2002.